Grafting of a High-Affinity Zn(II)-Binding Site on the β-Barrel of Retinol-Binding Protein Results in Enhanced Folding Stability and Enables Simplified Purification†

Holger N. Müller and Arne Skerra*

Max-Planck-Institut für Biophysik, Abteilung Molekulare Membranbiologie, Heinrich-Hoffmann-Strasse 7, D-60528 Frankfurt am Main, Germany

Received May 23, 1994; Revised Manuscript Received September 6, 1994⊗

ABSTRACT: In a rational protein design approach, the His_3 Zn(II)-binding site from the active center of human carbonic anhydrase II was transplanted on the β-barrel of mammalian serum retinol-binding protein (RBP) in a solvent-accessible location on the protein's outer surface. Several mutants of RBP were generated and produced in *Escherichia coli*, and their Zn(II)-binding properties were investigated in equilibrium dialysis experiments. One mutant, $RBP/H_3(A)$, with His residues introduced at the positions 46, 54, and 56 in the polypeptide sequence was shown to bind Zn(II) specifically with a stoichiometry of 1 and a corresponding dissociation constant equal to 36 ± 10 nM. Binding of Zn(II) had no influence on the binding of retinoic acid, a natural ligand of RBP. In guanidinium chloride-induced unfolding experiments the mutant was found to be significantly stabilized in the presence of small concentrations of $ZnSO_4$. This effect could be quantitatively explained using thermodynamic theory. Furthermore, it was demonstrated that the protein-bound Zn(II) is accessible to iminodiacetic acid as an additional chelating ligand without competition for the metal ion. Thus it was possible to use the grafted metal-binding site for the efficient purification of the engineered, bifunctional RBP via immobilized metal affinity chromatography from the bacterial protein extract.

The mammalian serum retinol-binding protein (RBP)[1] was the first member of the lipocalin family of proteins (Pervaiz & Brew, 1987) whose crystal structure was solved at high resolution (Cowan et al., 1990; Newcomer et al., 1984). RBP shows a simple folding architecture with a barrel of eight anti-parallel β-strands as the central motif. The β-barrel supports four loops at its upper end which form the entrance to the binding pocket for the hydrophobic ligand. Whereas the β-barrel is structurally highly conserved among the lipocalins, the loop regions show large differences between individual members and give rise to the variety of observed binding specificities. Despite their small size, the lipocalins are thus reminescent of immunoglobulins with their conserved structural framework and the hypervariable loops that make up binding sites for a huge number of different antigens. Therefore the lipocalins constitute a promising model system for the study of molecular recognition by proteins.

Due to its important physiological role in the transport of the vitamin A alcohol, RBP was subject to detailed biochemical investigation [for a recent review see Soprano and Blaner (1994)]. Several independent crystal structures of both the apo- and the holoprotein from different species were described (Cowan et al., 1990; Zanotti et al., 1993a,b). Consequently, RBP appears particularly attractive for protein engineering studies, and an *Escherichia coli* expression system for the functional protein was established (Müller & Skerra, 1993). Initially a flexible carboxy-terminal extension of six consecutive His residues was employed for the isolation of the recombinant RBP from the bacterial cell extract via IMAC.

Oligo-His affinity tails have gained increasing popularity for the purification of recombinant proteins since the work of Hochuli et al. (1988). Yet, a number of practical disadvantages may be encountered, including immunogenic side effects, heavy metal-induced protein precipitation, and interference with crystal growth for X-ray structural analysis. Removal of the oligo-His extension via proteolytic cleavage was suggested but has not been demonstrated in a routine application and would certainly complicate the isolation of a homogeneous recombinant gene product. Furthermore, in the case of RBP we are interested in studying the influence of the amino- and carboxy-terminal polypeptide segments, which protrude from the β-barrel, on the structure and function of the protein, so that the presence of an additional affinity tail might interfere.

Therefore, as a first step in the engineering of RBP, we removed the His_6 tail from the recombinant protein (Müller & Skerra, 1993) and tried to introduce a structurally defined metal ion binding site on the surface of its β-barrel instead. The observation that a Zn(II) ion is tightly bound in the active center of carbonic anhydrase by three His residues that are located on two adjacent anti-parallel β-strands (Liljas et al., 1994) prompted us to the notion that the same motif might be transferred to a segment of similar secondary structure

† This work was supported by the Deutsche Forschungsgemeinschaft.

* Corresponding author; Phone: +49 69 96769 389; Fax: +49 69 96769 423.

⊗ Abstract published in *Advance ACS Abstracts,* November 1, 1994.

[1] Abbreviations: A_{280}, absorption at 280 nm; CA2, human carbonic anhydrase II; EDTA, ethylenediaminetetraacetic acid; GdnHCl, guanidinium chloride; HEPES, *N*-(2-hydroxyethyl)piperazine-*N*′-2-ethanesulfonic acid; IDA, iminodiacetic acid; SDS, sodium dodecyl sulfate; IPTG, isopropyl-β-D-thiogalactopyranoside; IMAC, immobilized metal affinity chromatography; kDa, kilodaltons; K_d, dissociation constant; λ_{Ex}, excitation wavelength; λ_{Em}, emission wavelength; NTA, nitrilotriacetic acid; PAGE, polyacrylamide gel electrophoresis; PCR, polymerase chain reaction; RBP, retinol-binding protein; rms, root mean square; Tris, tris(hydroxymethyl)aminomethane.

0006-2960/94/0433-14126$04.50/0

in RBP. Since large parts of its β-barrel are solvent-exposed, the possibility existed that the grafted metal complexation site would permit interaction of the bound metal ion with the chelating groups of an IMAC column and thus serve for the isolation of the protein. In the present paper, we describe the successful design and characterization of such a Zn(II)-binding site on the surface of RBP.

EXPERIMENTAL PROCEDURES

Molecular Modeling. The atomic coordinates of the crystal structures of SCN^--inhibited human carbonic anhydrase II at 1.9 Å (Eriksson et al., 1988b) and of human serum RBP complexed with retinol at 2.0 Å (Cowan et al., 1990) were obtained from the Brookhaven Protein Data Bank (Bernstein et al., 1977). INSIGHT interactive graphics software (Biosym Technologies, Inc., San Diego, CA) was used for analysis and comparison of the structures and for the preparation of Figure 1. During superposition of the structural fragment comprising the His_3 Zn(II)-binding site in CA2 with corresponding parts of the β-barrel structure of RBP rms difference values were calculated with the same software using either the C_α and C_β coordinates of the three His residues 94, 96, and 119 in CA2 or the C_α coordinates of residues 93−97 and 118−120.

Construction of Mutants. Manipulation of nucleic acids was performed according to standard methodology (Sambrook et al., 1989). Single-stranded plasmid DNA was isolated, and site-directed mutagenesis was carried out as described by Geisselsoder et al. (1987). Oligodeoxynucleotides were prepared using an Applied Biosystems automated DNA synthesizer. Restriction enzymes, T4 DNA ligase, and T4 DNA polymerase were purchased from New England Biolabs (Schwalbach, Germany) or Boehringer Mannheim (Germany). For construction of the bacterial expression plasmid, the porcine RBP structural gene was PCR-amplified from the earlier described vector pHNM1 (Müller & Skerra, 1993) using the primers 5′-AGC GGA TAA CAA TTT CAC ACA GGA-3′ and 5′-TCT TTC AGC GCT CGG CGG ACA GTA ACC ATT GTG AGT-3′. The PCR product was purified on an agarose gel, digested with *Xba*I and *Eco*47III and ligated to the *Xba*I/*Eco*47III-cut vector fragment of pASK60-Strep (Schmidt & Skerra, 1993), yielding pHNM10.

The gene for a partially humanized version of the protein, which served as wild-type RBP in this study, was generated by mutagenesis (Asn50 → Thr; His52 → Gln) using the oligodeoxynucleotide 5′-CGT GGC GCT CAT CTG GCC GGT CTC GTC CAC GGA-3′. Remaining differences to human RBP were Ile107 (Val), Gln123 (Leu), Ala138 (Ser), His142 (Asn), Phe144 (Leu), Ser145 (Pro), Val148 (Ala), and Thr169 (Val) with the corresponding residues of human RBP in parentheses. The oligodeoxynucleotide 5′-TCG ACC CTT GGC GTG GGC GTG CAT CTG GCC GGT CTC GTC CAC GTG GAA TTC GGC GAC-3′ was used for the same purpose and for concomitant introduction of the substitutions Ser46 → His, Ser54 → His, and Thr56 → His, yielding RBP/H_3(A). Mutagenesis of the original gene with the oligodeoxynucleotide 5′-TAC GCC CCA GTA GTG CAT CTT GAA CTT GGC AGG GTC CTC GGT GTC GTG AAA GTG GCC CAC CAT GTC-3′ led to the substitutions Thr76 → His, Thr78 → His, and Lys89 → His and thus to the mutant RBP/H_3(B)+H. RBP/H_3(B) was obtained from RBP/H_3(B)+H using the oligodeoxynucleotide 5′-CGT GGC GCT CAT CTG GCC GGT CTC GTC CAC GGA-3′ for introduction of the substitutions Asn50 → Thr and His52 → Gln as above. An additional mutant, RBP/H_2(B)+H, which lacked the substitution Thr76 → His, was obtained unintentionally during construction of RBP/H_3(B)+H. All constructs were confirmed by plasmid dideoxy sequencing (Tabor & Richardson, 1987).

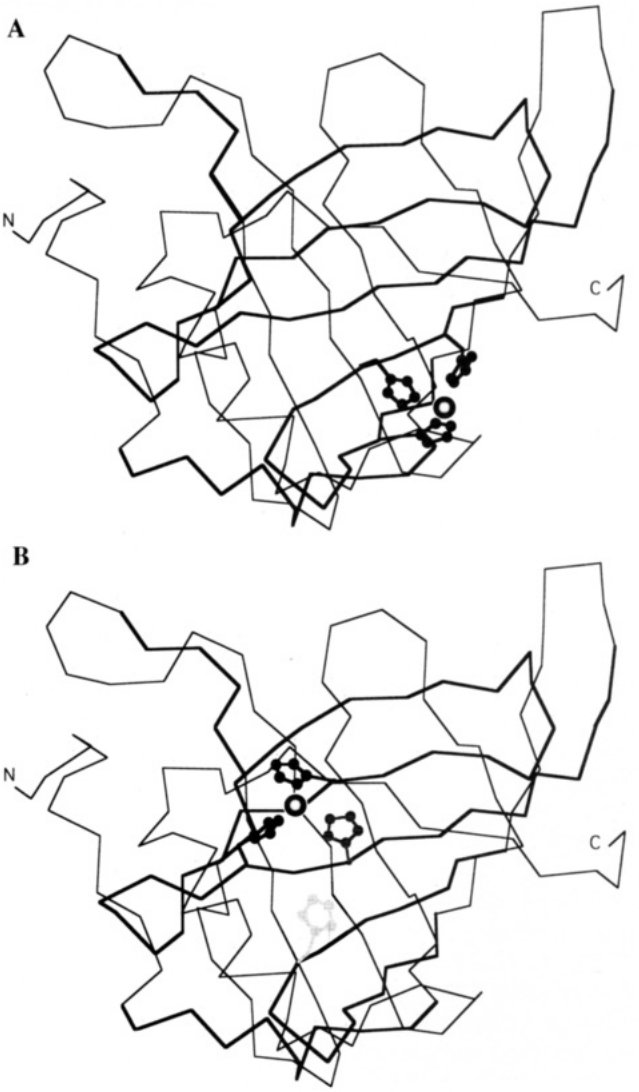

FIGURE 1: C_α drawing of RBP (Cowan et al., 1990), residues 1−174, with the His_3 Zn(II)-binding site grafted from CA2 (Eriksson et al., 1988b). The His side chains were introduced via superposition of their C_α and C_β atoms (cf. Table 1). They are shown with the atoms of the imidazole rings represented as spheres and the bound metal ion as a shaded ball, respectively. Retinol, the natural ligand of RBP, occupies a central cavity in the upper part of the β-barrel and was omitted. (A) Grafted Zn(II)-binding site (A), positions 46, 54, and 56 in RBP. (B) Grafted Zn(II)-binding site (B), positions 76, 78, and 89 in RBP. The additional residue His52, which is present in the mutants RBP/H_3(B)+H and RBP/H_2(B)+H (cf. Table 2), is shown in gray with a common side chain conformation (Ponder & Richards, 1987). Residue His76, which is missing in the mutants RBP/H_2(B) and RBP/H_2(B)+H, is shown in dark gray.

Recombinant Protein Production. Expression of the wild-type and mutant RBP genes was carried out in *E. coli* K12 strain JM83 (*ara*, Δ(*lac-pro*AB), *rps*L (= *str*A), Φ80, *lac*ZΔM15) (Yanisch-Perron et al., 1985) harboring the protein folding helper plasmid pASK61 similarly as described before (Müller & Skerra, 1993). In order to increase the amount of synthesized protein, induction with 1 mM IPTG

(Biomol, Ilvesheim, Germany) was extended from 3 h to overnight. Cells were harvested by centrifugation and resuspended in ice-cold cell fractionation buffer (500 mM sucrose, 100 mM NaCl, 50 mM Tris−HCl (pH 7.5), 1 mM EDTA). After being stirred for 30 min at 4 °C, the spheroplasts were removed by centrifugation, and the supernatant was recovered as the periplasmic cell fraction. The protein solution was dialyzed against CP buffer (1 M NaCl, 40 mM NaP_i, pH 7.5) and applied to a Ni(II)-charged column of Chelating Sepharose Fast Flow (Pharmacia, Freiburg, Germany). After being washed with CP buffer, bound protein was eluted in one step with 300 mM imidazole (Merck, Darmstadt, Germany). The solution was adjusted to 1 mM EDTA and dialyzed against SA buffer (100 mM Tris−HCl pH 8.0). The recombinant protein was then purified via the *Strep tag* affinity peptide on a column of streptavidin sepharose (10 mg of immobilized protein/mL). Homogeneous protein was eluted with 2.5 mM diaminobiotin (Sigma, Deisenhofen, Germany) dissolved in SA buffer as described (Schmidt & Skerra, 1994). For the removal of divalent metal ions the protein solution was adjusted to 100 μM EDTA and dialyzed three times against 50 mM NaP_i, pH 7.5, and once against KSH buffer (50 mM K_2SO_4, 20 mM HEPES (Roth, Karlsruhe, Germany) pH 7.5). All buffers were prepared in 0.05 μS water from a Milli Q (Millipore, Eschborn, Germany) purification system. Dialysis tubing and membranes (Spectra/Por 1, Spectrum Medical Industries, Inc., Los Angeles) were made metal-free according to Veillon and Vallee (1978). The yield of the recombinant protein was between 0.4 and 0.75 mg/L of *E. coli* culture. Purity was checked in 15% SDS/PAGE (Fling & Gregerson, 1986) followed by staining with Coomassie brilliant blue. For protein concentration determination a molar extinction coefficient of 44 950 M^{-1} cm^{-1} obtained according to Scopes (1974) was used for all mutants. Recombinant expression, purification, and concentration determination of the RBP-His_6 variant were performed as previously described (Müller & Skerra, 1993). Fluorescence titration with retinoic acid in KSH buffer and analysis of the data were also carried out following the earlier published protocols.

Zn(II) Equilibrium Dialysis. Equilibrium dialysis experiments were carried out in self-made acrylic vessels with two adjacent 500 μL compartments, which were separated by a metal-free dialysis membrane. For each point of the Zn(II)-binding curve, one compartment was filled with 400 μL of the protein solution (2.5−8 μM) in KSH buffer, and the opposite compartment was filled with 400 μL of the buffer containing $ZnSO_4$ at an appropriate concentration. Binding of Zn(II) to unfolded protein was measured in the presence of 5 M GdnHCl (USB, Cleveland, OH) under otherwise unchanged buffer conditions, after RBP/H_3(A) or wild-type RBP had been completely denatured in a preincubation for 16 h. Following equilibration overnight at 22 °C with gentle agitation, the Zn(II) concentration was determined in both compartments using a PYE/UNICAM SP9 (Pye Unicam Ltd, Cambridge, England) atomic absorption spectrophotometer with an acetylene-air flame. The atomic absorbance was measured at 213.9 nm with the bandwidth set to 0.5 nm. A standard solution of $ZnSO_4$ was gravimetrically prepared and diluted in KSH buffer at concentrations in the range between 0 and 30 μM. Prior to measuring Zn(II) in the presence of GdnHCl a constant concentration of 5 μM Zn(II) was added to all samples (and the same value later subtracted) since concentrations below 4 μM Zn(II) could not be precisely determined due to physical interferences with the flame. For Zn(II)-binding experiments in the presence of NTA (Fluka, Neu-Ulm, Germany) or IDA (SIGMA, Deisenhofen, Germany), the chelator compound was added at 200 μM to the protein solution, which was then used for equlibrium dialysis as above. IDA was purified by recrystallization from hot water for this purpose. Nevertheless, a small offset of 187 nM was detected in the binding curve, corresponding to a 0.19 mol % contamination of IDA with a strong complex forming, EDTA-like compound that obviously masked a constant quantity of the Zn(II). Therefore, the measured Zn(II) concentrations in both compartments were corrected by this value prior to analysis of the data.

Analysis of Zn(II)-Binding Data. For an equimolar complex between Zn(II) and RBP, the dissociation constant, K_d, is defined by the equation of mass law

$$K_d = \frac{[RBP][Zn]}{[RBP{\cdot}Zn]}$$

where the concentration of the free ([Zn]) and bound ([RBP·Zn]) metal ion was obtained from equilibrium dialysis. With $[RBP]_T$ as the total protein concentration and $[RBP] = [RBP]_T - [RBP{\cdot}Zn]$, the following formula was deduced:

$$[RBP{\cdot}Zn] = \frac{[Zn][RBP]_T}{K_d + [Zn]} \quad (1)$$

Using nonlinear least-squares minimization (Kaleidagraph Software, Abelbeck, on an Apple Macintosh computer) both K_d and $[RBP]_T$ were fitted as parameters. Otherwise, even small errors in the experimental determination of the protein concentration would have impaired proper evaluation of the data.

When a stoichiometry of two bound Zn(II) ions per protein molecule was observed, two independent dissociation equilibria were assumed:

$$K_{d1} = \frac{[RBP][Zn]}{[RBP{\cdot}Zn]} \qquad K_{d2} = \frac{[RBP{\cdot}Zn][Zn]}{[RBP{\cdot}Zn_2]}$$

With the total concentration of RBP, $[RBP]_T = [RBP] + [RBP{\cdot}Zn] + [RBP{\cdot}Zn_2]$, and the concentration of bound Zn(II), $[Zn]_b = [RBP{\cdot}Zn] + 2\,[RBP{\cdot}Zn_2]$, the following equation was deduced and used for fitting the data:

$$[Zn]_b = \left(1 + \frac{2[Zn]}{K_{d2}}\right)\frac{[RBP]_T}{\frac{K_{d1}}{[Zn]} + 1 + \frac{[Zn]}{K_{d2}}} \quad (2)$$

In this case K_{d1} and K_{d2} were used as free parameters.

For the preparation of Figures 2 and 4, the ratio $[RBP{\cdot}Zn]/[RBP]_T$ was plotted against [Zn] in the case of eq 1, and the ratio $[Zn]_b/[RBP]_T$ was plotted against [Zn] in the case of eq 2 (see figure legends).

Equilibrium Denaturation. For each point of the unfolding curve, 50 μL of a 10 μM protein solution in KSH buffer was mixed with 450 μL of the buffer containing a given concentration of GdnHCl and supplemented with either $ZnSO_4$ or EDTA (see text). The sample was incubated to equilibrium overnight at 22 °C, and fluorescence was

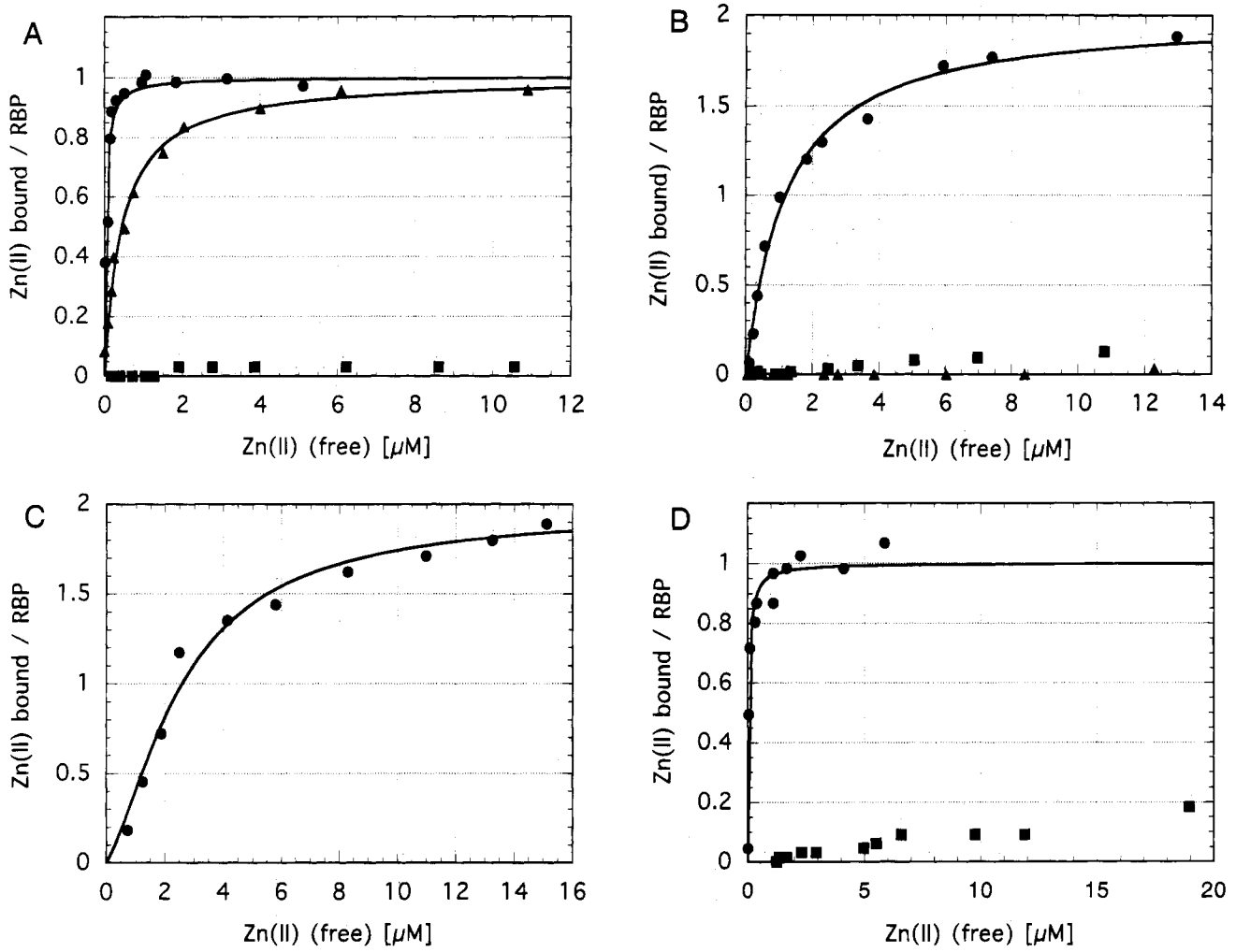

FIGURE 2: Zn(II)-binding curves from equilibrium dialysis experiments. The molar ratio of bound Zn(II) per protein is plotted vs the concentration of uncomplexed Zn(II). The corresponding calculated K_d values are given in Table 2. (A) Data for RBP/H_3(A) (filled circles), 8 μM, RBP/H_3(B) (filled triangles), 7 μM, and wild-type RBP (filled squares), 7 μM. The continuous lines represent least-squares fits according to eq 1. The calculated protein concentrations were 9.1 μM for RBP/H_3(A) and 7.3 μM for RBP/H_3(B). (B) Data for RBP/H_2(B) (filled triangles), 7 μM, RBP/H_2(B)+H (filled squares), 7 μM, and RBP/H_3(B)+H (filled circles), 7 μM. The continuous line for RBP/H_3(B)+H represents a least-squares fit according to eq 2. (C) Data for RBP-His_6 (closed circles), 2.3 μM, fitted according to eq 2. (D) Data for RBP/H_3(A), 7 μM, in the presence of 100 μM NTA (filled squares) and RBP/H_3(A), 8 μM, in the presence of 100 μM IDA (filled circles). The continuous line in the case of IDA represents a least-squares fit according to eq 1 with a calculated protein concentration of 8.1 μM.

measured using excitation at 295 nm and emission at 325 nm in a Perkin Elmer LS50 fluorimeter as described (Müller & Skerra, 1993). The exact concentration of GdnHCl in the samples was determined by measuring the refractive index of the solution (Pace, 1986) with an Abbe refractometer (Zeiss, Oberkochen, Germany).

Analysis of Equilibrium Denaturation Data. The measured data were evaluated according to the six-parameter algorithm described by Santoro and Bolen (1988) using nonlinear least-squares minimization (Kaleidagraph Software, Abelbeck, on an Apple Macintosh computer). As result, values for $\Delta G^0_{n\text{-}u}$, the Gibbs free energy of unfolding extrapolated to the absence of denaturant, and m, the parameter for the cooperativity of the transition, were obtained. In order to calculate the concentration of denaturant at which 50% of the protein was unfolded, $[D]_{1/2}$, the relation $\Delta G^0_{n\text{-}u} = m[D]_{1/2}$ was used. For comparison of two mutants or two different unfolding conditions, I and II

$$\Delta\Delta G_u = 0.5(m^I + m^{II})([D]^I_{1/2} - [D]^{II}_{1/2}) \quad (3)$$

was calculated as the difference in free energy of unfolding in the presence of denaturant (Kellis et al., 1989). In this way large deviations during extrapolation to zero denaturant concentration resulting from small errors in m were avoided.

IMAC Purification of the Zn(II)-Binding RBP Mutant. One-step IMAC purification was performed on a column (785 mm^2 × 51 mm) containing 4 mL of Chelating Sepharose Fast Flow (Pharmacia, Freiburg, Germany) charged with Ni(II). After equilibration with CP buffer, 10 mL of periplasmic protein extract, prepared after 3 h induction with 0.5 mM IPTG from 1 L *E. coli* culture (see above), was applied (flow rate 36 mL/h). The column was washed with CP buffer and a gradient (120 mL) between 0 and 100 mM imidazole in CP buffer was used for elution of the protein (flow rate 18 mL/h).

RESULTS

Grafting of the Zn(II)-Binding Site from Human Carbonic Anhydrase II on the β-Barrel of RBP. In CA2 three His side chains, 94, 96, and 119, which protrude from two

Table 1: Superposition of the His_3 Zn(II)-Binding Site from CA2 (Erikkson et al., 1988b) on the β-Barrel Structure of RBP (Cowan et al., 1990)

mutant	location in RBP[a]	5 + 3 C_α positions,[b] rms difference (Å^2)	3 C_α-C_β pairs,[c] rms difference (Å^2)
RBP/H_3(A)	54/56/46	0.46	0.34
RBP/H_3(B)	76/78/89	0.52	0.27
	42/44/58	0.52	0.44
	56/58/44	0.59	0.57
	87/89/78	0.69	0.57

[a] Positions in the polypeptide sequence at which the three His residues would be introduced. [b] The C_α atoms of the three His residues and their immediate neighbors in CA2 (93−97 and 118−120) were used for least-squares superposition to RBP. [c] Only the C_α and C_β atoms of the three His residues in CA2 (94, 96, and 119) were superimposed with corresponding atomic positions in RBP.

hydrogen-bonded, anti-parallel β-strands, serve as ligands for the bound Zn(II) ion. Whereas in the native structure the metal ion is tetrahedrally coordinated, with one water molecule occupying the fourth ligand position (Eriksson et al., 1988a), Zn(II) exhibits an expanded coordination shell with almost octahedral geometry in the SCN^--inhibited enzyme (Eriksson et al., 1988b). In order to allow for enhanced ligand accessibility of the bound Zn(II) ion the atomic positions of the metal binding site were extracted from the latter crystal structure and used for comparison with RBP (Cowan et al., 1990).

The C_α positions of the three His residues plus their immediate neighbors in the polypeptide chain of CA2 (i.e., positions 93−97 and 118−120) were superimposed in a stepwise fashion along the β-strand pairs B/C and D/E, respectively, of RBP. During this procedure the local symmetry of the anti-parallel β-strand pairing was taken into account so that always two perpendicular mutual orientations with equivalent backbone hydrogen-bonding were investigated. Altogether 44 potential binding site positions in RBP were analyzed, and corresponding rms differences were calculated. Five positions were found with values below 0.7 Å, indicating high similarity in the fine structure and local curvature of the β-strands (Table 1). In order to make use of the side chain orientations as a second criterion, another superposition was done between the C_α- and C_β-coordinates of the three His residues in CA2 and those of the corresponding residues in RBP (cf. Table 1). As result, two potential ligand sites, designated (A) and (B), were identified in RBP that permitted the introduction of three His residues on a structural backbone with very similar conformation as in CA2. Figure 1 shows a C_α-plot of RBP together with the superimposed His_3 Zn(II)-binding site from CA2 for the two locations. In both cases the His side chains are well exposed to the solvent, and the bound metal ion can be approached by additional ligands.

In order to experimentally characterize the RBP mutants with the grafted Zn(II)-binding site, a recently described system (Müller & Skerra, 1993) for the production of functional porcine serum RBP in *E. coli* was employed. This protein differed in 10 amino acid positions from human RBP, whose structure was used for the modeling, and had a His_6 tail fused to its carboxy-terminus. For the purification of all RBP mutants investigated here under identical conditions, the His_6-tail was replaced by the *Strep tag* affinity peptide (Schmidt & Skerra, 1993). Residues 175−183 of RBP, which do not exhibit a defined conformation in the crystal structures reported so far (Cowan et al., 1990; Zanotti et al., 1993a,b), were deleted during this step. The resulting protein could be affinity-purified to homogeneity on streptavidin sepharose as demonstrated before (Schmidt & Skerra, 1994).

Table 2: Definition and Zn(II)-Binding Properties of RBP Mutants Generated in This Work

mutant	amino acid substitutions[a]	K_d[b]
wild-type RBP[c]		—[d]
RBP/H_3(A)	His46(Ser) His54(Ser) His56(Thr)	36 ± 10 nM
RBP/H_3(B)	His76(Thr) His78(Thr) His89(Lys)	440 ± 48 nM
RBP/H_2(B)	His78(Thr) His89(Lys)	—[d]
RBP/H_2(B)+H	His78(Thr) His89(Lys) His52(Gln) Asn50(Thr)	—[d]
RBP/H_3(B)+H	His76(Thr) His78(Thr) His89(Lys) His52(Gln) Asn50(Thr)	650 ± 100 nM 2.1 ± 0.3 μM
RBP-His_6[e]		3.6 ± 1.2 μM 1.9 ± 0.6 μM

[a] Original residues in the wild-type RBP are given in parentheses. [b] Dissociation constant for the binding of Zn(II) determined by equilibrium dialysis. [c] Recombinant porcine RBP as described by Müller and Skerra (1993) with the amino acid sequence ProProSerAlaTrpArg-HisProGlnPheGlyGly added after residue 174 and the substitutions Asn50 → Thr and His52 → Gln. [d] No measurable Zn(II) affinity was detected. [e] Recombinant porcine RBP with a His_6 extension after residue 183 (Müller & Skerra, 1993).

In the structural gene for RBP, two out of the 10 amino acid positions which differed from the human protein, Asn50 and His52, were located in proximity to the putative Zn(II)-binding sites described above. In order to avoid a local structural change compared with the crystal coordinates of the human protein or functional interference by the additional His residue (cf. Figure 1B), both positions were changed to the human amino acids Thr and Gln, respectively. All RBP mutants that were produced in this study are listed in Table 2 (see also Experimental Procedures).

Zn(II)-Binding Properties of RBP Mutants. Zn(II) affinities were measured in equilibrium dialysis experiments, and the corresponding K_d values were calculated from free and bound Zn(II) concentrations determined by atomic absorption spectrometry. Figure 2A shows the data for the mutants RBP/H_3(A) and RBP/H_3(B) in comparison with wild-type RBP. Whereas in the case of wild-type RBP no binding of Zn(II) was detectable, RBP/H_3(A) exhibited high affinity for Zn(II) with a K_d of 36 ± 10 nM and RBP/H_3(B) showed an affinity that was approximately 10-fold lower (Table 2). Both mutants bound the metal ion with a stoichiometry of 1 since measured protein concentration and the corresponding value calculated from the curve fit of the equilibrium dialysis data (see Experimental Procedures) agreed within 17% (in respect to the former).

The influence of the topographical arrangement of the His residues introduced into RBP was investigated using the variants of Zn(II)-binding site (B) that are listed in Table 2.

Zn(II) affinity was completely lost (Figure 2B) if the single His residue at position 76 was removed in the mutant RBP/H_2(B). Introduction of another His residue on a neighboring β-strand instead (His52, see Figure 1B), yielding RBP/H_2-(B)+H, did not restore Zn(II)-binding capability (Figure 2B). However, when the original mutant RBP/H_3(B) was supplied with the same additional His residue a second Zn(II)-binding site was created. Analysis of the data for this mutant, RBP/H_3(B)+H, clearly revealed the binding of two Zn(II) ions instead of one (Figure 2B). Two different K_d values were calculated in this case (Table 2), pointing toward one Zn(II)-binding site with similar properties as in RBP/H_3(B) and a second one with slightly lower affinity.

In order to compare the chelating properties of the structurally defined Zn(II)-binding sites created here with a simple oligo-His tail, as it has been frequently used for the purification of recombinant proteins via IMAC, equilibrium dialysis experiments were carried out with the earlier described RBP-His_6 protein (Müller & Skerra, 1993). In this case a stoichiometry of two bound Zn(II) ions was observed in the range of metal ion concentration investigated (Figure 2C). The two calculated dissociation constants were almost identical and in the low micromolar range (Table 2).

For the IMAC purification of proteins, two different affinity matrices are commercially available, one carrying an IDA ligand (Chelating Sepharose Fast Flow, Pharmacia, Freiburg, Germany) and one with an immobilized NTA derivative (Ni-NTA Agarose, Diagen, Düsseldorf, Germany). In order to study Zn(II) complexation by the grafted binding site in the presence of one of these chelating compounds, corresponding equilibrium dialysis experiments were carried out for the high-affinity mutant RBP/H_3(A). No metal ion binding to the protein could be detected in the presence of an excess amount of NTA (Figure 2D). However, with the addition of 100 μM IDA an essentially unaffected binding curve was observed (Figure 2D) compared with the data in the absence of the chelating compound (cf. Figure 2A). The calculated dissociation constant for RBP/H_3(A) was 44 $\pm$ 8 nM under these circumstances and thus indistinguishable from the K_d for the binding of uncomplexed Zn(II) (Table 2).

Effect of Zn(II)-Binding on Folding Stability. The influence of Zn(II) complexation by the high-affinity mutant RBP/H_3(A) on its stability against unfolding was investigated via GdnHCl-induced equilibrium denaturation. Reversible unfolding of RBP is accompanied by a sharp decrease in the intrinsic tryptophan fluorescence and shows a simple two-state behavior (Müller & Skerra, 1993). The fluorescence properties in the native and denatured state, respectively, were found to be essentially identical between wild-type RBP and the mutant as well as Zn(II)-bound RBP/H_3(A). The normalized denaturation curves either under metal-free conditions or in the presence of excess concentrations of Zn(II) are depicted in Figure 3.

Whereas in the absence of Zn(II) wild-type RBP and RBP/H_3(A) displayed almost precisely the same unfolding transition—although with slightly different values derived for m—the Zn(II)-binding mutant was significantly stabilized in the presence of the metal ion (Table 3). The wild-type protein was marginally destabilized with an increasing Zn(II) concentration and, similarly, RBP/H_3(A) exhibited the higher $D_{1/2}$ value of 2.53 M GdnHCl in the presence of 10 μM Zn(II) compared with a metal concentration of 100 μM.

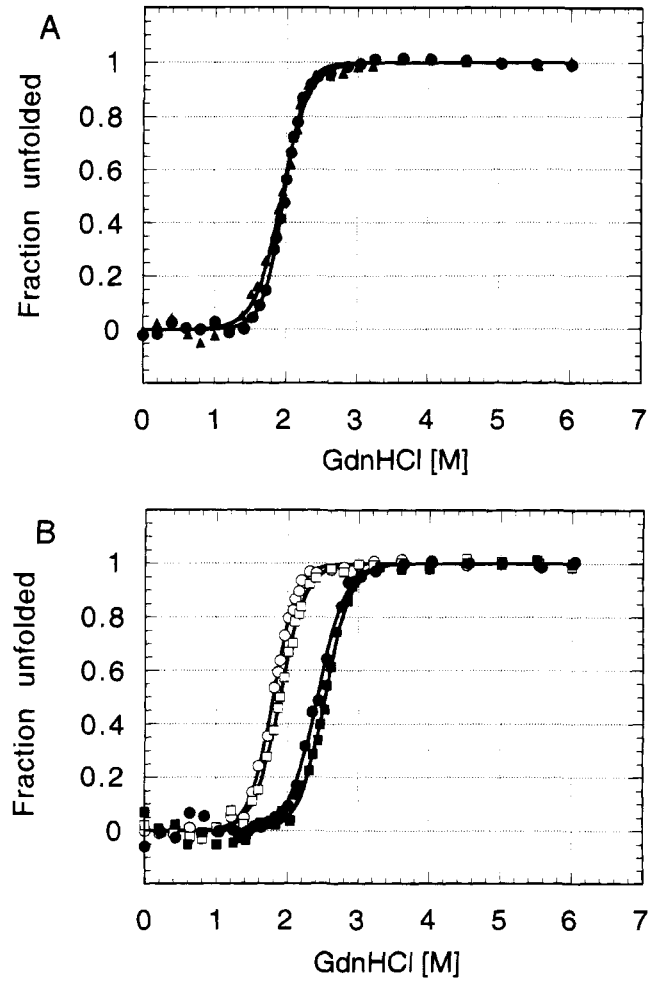

FIGURE 3: Influence of Zn(II) on the GdnHCl-induced unfolding transitions of wild-type RBP and RBP/H_3(A). (A) Plot of the fraction unfolded for RBP (filled triangles) and RBP/H_3(A) (filled circles) vs the concentration of denaturant in the presence of EDTA. (B) Analogous denaturation plot for RBP (open symbols) and RBP/H_3(A) (filled symbols) in the presence of 10 μM Zn(II) (squares) or 100 μM Zn(II) (circles).

Analogous unfolding experiments were performed with RBP/H_3(A) using 10 or 100 μM of the Zn(II)-IDA complex. The resulting $D_{1/2}$ concentrations were 2.52 $\pm$ 0.01 and 2.48 $\pm$ 0.01 M GdnHCl, respectively, and thus essentially indistinguishable from those in the absence of the chelating compound.

From the calculation of ΔG_u differences in the presence of denaturant (see Experimental Procedures) RBP/H_3(A) showed a stabilization by up to 8.5 kJ/mol in the Zn(II)-complexed state compared with metal-free conditions (see Table 3). The small destabilizing contribution with increasing Zn(II) concentration described above was cancelled out when the free energy difference was calculated between RBP/H_3(A) and the wild-type protein at identical conditions (Table 3, last column). In the metal-free state $\Delta\Delta G_u$ became negligible, but in the presence of Zn(II) the mutant was more stable than wild-type RBP by approximately 8.6 kJ/mol, irrespective whether 10 or 100 μM Zn(II) was present.

Since the relative stabilization of Zn(II)-complexed RBP/H_3(A) was thus not dependent on the metal ion concentration in the range investigated, thermodynamic considerations led to the presumption that the denatured mutant displayed Zn(II)-binding capability with measurable affinity as well (for a detailed discussion see Appendix). Therefore, Zn(II)

Table 3: Parameters for the Reversible Unfolding of RBP and RBP/H_3(A) in the Absence or Presence of Zn(II) during GdnHCl-Induced Denaturation

protein	Zn(II) (μM)	m^a (kJ mol^{-1} M^{-1})	$\Delta G^0_{n-u}{}^b$ (kJ mol^{-1})	$D_{1/2}{}^c$ (M)	$\Delta\Delta G_u{}^d$ (kJ mol^{-1})	$\Delta\Delta G_u{}^e$ (kJ mol^{-1})
RBP	–[f]	13.2 ± 1.0	25.7 ± 2.0	1.94 ± 0.02		
	10	13.7 ± 0.6		1.90 ± 0.01	−0.5	
	100	15.1 ± 0.6		1.80 ± 0.01	−2.0	
RBP/H_3(A)	–[f]	16.6 ± 0.7	32.8 ± 1.5	1.97 ± 0.01		0.5
	10	13.9 ± 1.0		2.53 ± 0.01	8.5	8.7
	100	12.5 ± 0.8		2.42 ± 0.01	6.6	8.6

[a] m is the parameter for the cooperativity of unfolding (see Experimental Procedures). [b] ΔG^0_{n-u} is the free energy of unfolding extrapolated to zero denaturant concentration. [c] $[D]_{1/2}$ is the concentration of GdnHCl at which 50% of the protein is unfolded. [d] Difference in free energy of unfolding (in the presence of denaturant) with reference to the metal-free state. [e] Difference in free energy of unfolding (in the presence of denaturant) between RBP/H_3(A) and RBP under the same experimental conditions. [f] Unfolding experiment with the addition of 50 μM EDTA.

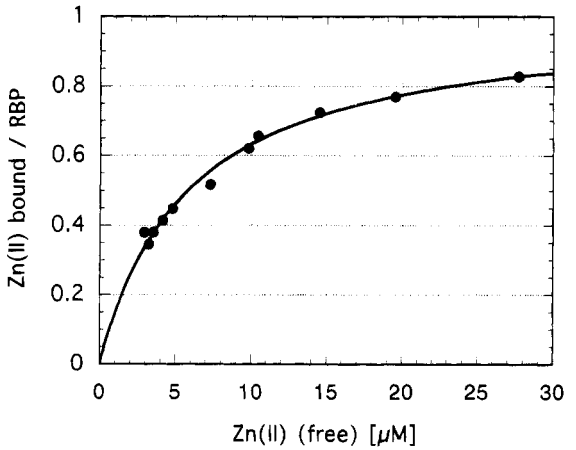

FIGURE 4: Zn(II)-binding curve for unfolded RBP/H_3(A), 7.6 μM, in the presence of 5 M GdnHCl determined by equilibrium dialysis. The continous line represents a least-squares fit according to eq 1 resulting in a calculated K_d value of 5.7 ± 0.4 μM. The calculated protein concentration was 9.1 μM in this case. Data points below ca. 3 μM free Zn(II) could not be measured due to the endogenous Zn(II) content of the GdnHCl solution.

equilibrium dialysis experiments were performed with the unfolded protein in the presence of 5 M GdnHCl. Whereas no binding could be detected for the wild-type RBP under these conditions (not shown) denatured RBP/H_3(A) exhibited Zn(II) affinity with a calculated dissociation constant of 5.7 ± 0.4 μM and a stoichiometry of 1 (Figure 4).

Use of the Grafted Zn(II)-Binding Site for IMAC Purification. When the periplasmic protein extract of an *E. coli* culture producing RBP/H_3(A) was applied to a Zn(II)-charged column of IDA sepharose, the protein was bound. However, during elution it was not well separated from some host proteins that also exhibited metal ion affinity (not shown). Excellent selectivity was achieved when the same column was charged with Ni(II). Under these circumstances RBP/H_3(A) gave rise to an additional peak in the imidazole gradient (Figure 5A) and was eluted in homogeneous form, whereas wild-type RBP could not be isolated (Figure 5B). RBP/H_3(A) thus IMAC-purified from the bacterial protein extract in a single step was indistinguishable in SDS/PAGE from the protein that was prepared using the *Strep tag* technique (Figure 5C).

Bifunctionality of the Zn(II)-Binding RBP Mutant. The bacterially produced recombinant RBP was previously shown to be fully functional in the binding of *all-trans*-retinoic acid, a derivative of the natural ligand retinol, compared with the native human protein (Müller & Skerra, 1993). In order to study the influence of Zn(II) complexation on the binding of retinoic acid by the mutant RBP/H_3(A), fluorescence titration experiments were carried out with this ligand in the absence or presence of Zn(II) (Figure 6). The two binding curves were almost identical, and a least-squares fit of the data resulted in a K_d value of 0.10 ± 0.02 μM under metal-free conditions compared with 0.15 ± 0.02 μM in the presence of 100 μM Zn(II). In the case of the wild-type RBP (from this study), the titration curves with and without Zn(II) were essentially indistinguishable (not shown) giving rise to K_d values of 0.12 ± 0.03 and 0.09 ± 0.02 μM, respectively.

DISCUSSION

In the active center of human carbonic anhydrase II the Zn(II)-binding site is formed by three imidazole groups, which protrude into a water-filled cavity of the protein, where the fixed Zn(II) ion serves as an electrophilic catalyst in the hydration of CO_2 (Liljas et al., 1994). One would expect that the precise side chain conformations of the corresponding His residues are not only determined through the local secondary structure of the underlying polypeptide backbone but also through packing interactions with neighboring residues in the interior of the folded protein. When the Zn(II)-binding site was grafted on RBP the three His residues became displayed on the convex protein surface of its β-barrel. As a consequence the introduced His residues were largely exposed to bulk solvent. Their side chain contacts were restricted to the few immediately neighboring residues on the bent β-sheet and not further optimized in this study. Nevertheless, the grafted binding site position (A) showed high affinity for the Zn(II) ion with a K_d of 36 ± 10 nM. Compared with a corresponding value in the picomolar range for native carbonic anhydrase (Lindskog & Nyman, 1964) this suggests that the fine structure of the framework which supports the imidazole side chains is indeed the major determinant. Accordingly, binding site position (B), which showed a decreased match during superposition of the structural elements, gave rise to a diminished Zn(II) affinity.

The plain stoichiometry of Zn(II) binding observed for both His_3 mutants of RBP, together with the finding that Zn(II) binding is abolished when one of the His residues was removed in the mutant RBP/H_2(B), makes clear that it is the tridentate character of the binding site which is responsible for the remarkable metal ion affinity. In how far the nature of those amino acid side chains which surround the Zn(II)-binding site in both mutants plays a role for its function remains to be elucidated in future protein engineering experiments or by structural analysis. Interestingly, a single additional His side chain located at an appropriate distance to binding site (B) was found to enable the complexation of a second Zn(II) ion with comparable affinity.

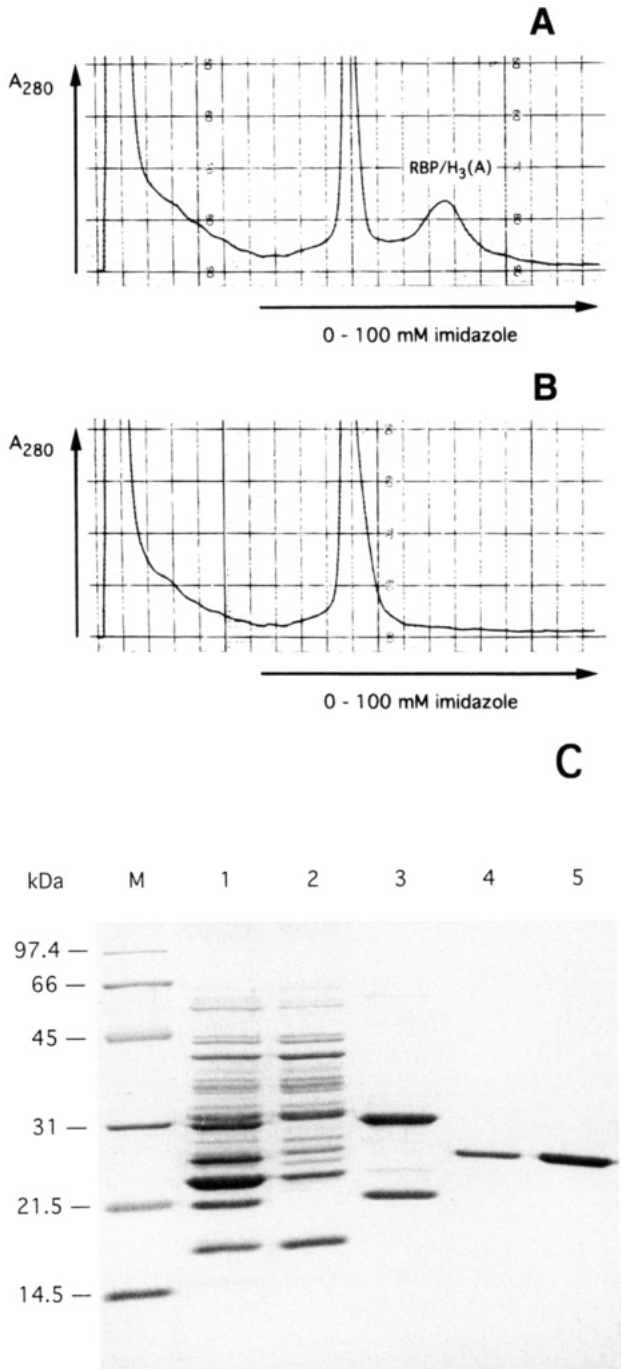

FIGURE 5: One-step purification of RBP/H_3(A) from the bacterial periplasmic protein extract by IMAC (see Experimental Procedures). (A) Elution profile monitored via A_{280} for RBP/H_3(A). The specific peak, which corresponds to the purified protein, is indicated. (B) Elution profile for wild-type RBP under identical conditions. (C) Coomassie-stained 15% SDS/PAGE corresponding to the chromatogram shown in (A) of the periplasmic cell extract (lane 1), flow through (lane 2) and the fraction of nonspecifically bound proteins eluted in the first peak (lane 3). RBP/H_3(A) from the second peak at higher imidazole concentration is shown in lane 4. For comparison, 1 μg of the same protein purified via the *Strep tag* technique is also shown (lane 5). M denotes the molecular size standard.

This finding underlines the cooperative effect in the chelating properties of the set of imidazole groups introduced into RBP.

As prerequisites for its use in the purification of the engineered RBP via IMAC the artificial Zn(II)-binding site had to be (i) accessible to a large immobilized ligand and

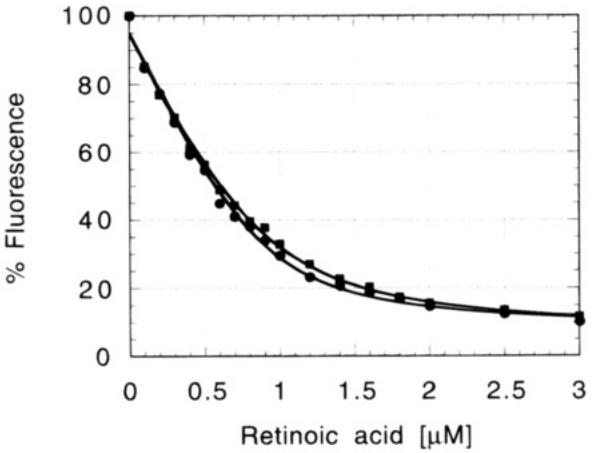

FIGURE 6: Fluorescence titration (λ_{Ex} = 295 nm, λ_{Em} = 340 nm) of RBP/H_3(A), 0.9 μM, with retinoic acid in the presence of 50 μM EDTA (filled circles) or with the addition of 100 μM Zn(II) (filled squares). The continuous lines represent least-squares fits for bimolecular complex formation (Müller & Skerra, 1993) resulting in K_d values of 0.10 ± 0.02 and 0.15 ± 0.02 μM, respectively.

(ii) able to accommodate additional coordinating groups without competition for the bound metal ion. Steric accessibility from the solvent was maintained by surface exposure of the His side chains on the outside of the β-barrel. However, in the native carbonic anhydrase structure the Zn(II) ion is tetrahedrally coordinated, and a single interchangeable ligand position would not permit the simultaneous complexation by a chelating group from the chromatography support. Although in Zn(II)-chelating proteins the ion generally prefers a coordination number of 4 (Christianson, 1991), Zn(II) is capable of octahedral coordination in aqueous solution. Therefore, it was sought to favor expansion of the coordination shell by choosing the template coordinates of the His ligands from the high-resolution crystal structure of the SCN^--inhibited carbonic anhydrase (Eriksson et al., 1988b). In this structure Zn(II) shows in fact octahedral coordination geometry with one missing position due to steric interference with the side chain of Thr199 in the enzyme's active site.

In the Zn(II)-binding experiments with RBP/H_3(A) it was observed that addition of the tridentate chelator IDA did not give rise to a measurable competition effect, although a concentration was used which was more than 3 orders of magnitude higher than the reported K_d of 58 nM for the IDA-Zn(II) complex (Martell & Smith, 1974). In contrast, the tetradentate chelating ligand NTA abolished Zn(II) binding to the protein completely. This leads to the conclusion that, when bound to the engineered RBP, the Zn(II) ion tolerates simultaneous complexation by the first compound, which resembles the immobilized ligand presented by IDA sepharose (Pharmacia's Chelating Sepharose Fast Flow). Indeed IMAC purification of RBP/H_3(A) was enabled by the grafted binding site, although the use of Ni(II) instead of Zn(II) gave rise to improved selectivity, permitting separation from all bacterial periplasmic proteins in a single step.

The introduction of His residues as metal ion coordination sites into proteins and their interaction with immobilized Cu(II) ions were reported earlier. In these examples, two His residues spaced by three intervening amino acids were incorporated into α-helices in the tertiary structures of cytochrome *c* and somatotropin, respectively (Arnold &

Haymore, 1991; Suh et al., 1991; Todd et al., 1991). However, the binding of Zn(II), which forms less stable complexes with imidazole ligands than Cu(II), was not shown. Work on a His_3 metal ion binding site grafted from carbonic anhydrase B on an immunoglobulin V_L domain (Iverson et al., 1990) was focused at the complexation of Cu(II) as well. An indication for the binding of Zn(II) was obtained in a competition assay pointing to a K_d likely in the 100 μM range. This weak affinity may be explained by steric restrictions due to the burial of the putative binding site at the interface between the V_L and V_H domains of the antibody, a feature that should also abolish its potential application for IMAC purification purposes.

Strong binding of Zn(II) was only achieved in one earlier protein design study using an artificial four helix bundle protein with a tetradentate Cys_2His_2 array (Regan & Clarke, 1990). In competition experiments with the Co(II)-complexed protein, a K_d of 25 nM was deduced for Zn(II), which is comparable to the value measured for the His_3 binding site introduced at position (A) into RBP here. Yet the tetrahedrally complexed Zn(II) ion would probably not be accessible to additional ligands in the four helix bundle protein. Furthermore, care had to be taken that the two Cys residues were kept in the reduced state prior to reconstitution of the metal complex. Therefore, the use of a Cys_2His_2 binding site would be difficult to adapt to proteins that must be secreted to an oxidizing cell compartment in order to form their disulfide bonds properly, as it is the case for RBP (Müller & Skerra, 1993).

Previous observations indicated that metal ion complexation by an engineered binding site can lead to stabilization against GdnHCl-induced denaturation as a consequence of preferential binding to the folded protein (Kellis et al., 1991; Regan & Clarke, 1990). A similar result was obtained here in unfolding experiments with the high-affinity mutant RBP/H_3(A). In the presence of Zn(II) the midpoint of unfolding was shifted by up to 0.56 M toward higher denaturant concentrations. Notably, the use of a Zn(II)-IDA complex led to precisely the same stabilization effect, which again suggests that Zn(II) can be chelated by the grafted His_3 binding site and IDA at the same time. Since the mere introduction of the three His residues into the β-barrel of RBP had no measurable effect, the stability against unfolding of the Zn(II)-complexed mutant protein was significantly enhanced compared with wild-type RBP [cf. also Müller and Skerra (1993)]. This contrasts to the behavior of the four helix bundle protein with the Cys_2His_2 site quoted above, where despite of a stabilizing metal chelation effect the metal-bound protein was still less stable than the unmodified protein [cf. Berg (1993)].

In RBP/H_3(A) the three His residues that form the metal binding site are displayed on two hydrogen-bonded β-strands. Consequently, Zn(II) should bind exclusively to the folded protein and thereby crosslink two adjacent strands of the β-barrel, which would explain the stabilizing effect. However, under such circumstances the measured relative increase in folding stability should be dependent on the Zn(II) concentration (see Appendix). Since this was not observed to be the case, a single Zn(II)-binding site with weaker affinity had to be postulated for the unfolded protein. Using the relation $\Delta\Delta G = \Delta G_A - \Delta G_A^U$ (see Appendix), together with a measured relative increase in the free energy of unfolding by 8.6 kJ/mol (see Table 3) and a dissociation constant of 36 nM for native RBP/H_3(A) (see Table 2), a K_d value of 1.2 μM was calculated for the binding of Zn(II) to the unfolded protein. This number is in close agreement with the dissociation constant of 5.7 μM determined by equilibrium dialysis in the presence of denaturant.

The precise nature of the Zn(II)-binding site in the unfolded protein, which is unique to RBP/H_3(A) and not present in the wild-type protein, remains however to be elucidated. In RBP/H_3(A) the three His residues were introduced at positions 46, 54, and 56 adjacent to a turn. In the light of the remarkable Zn(II)-binding properties of a simple flexible His_6 tail determined here it is conceivable that the mere proximity in the primary structure—together with potential liganding properties of neighboring amino acid side chains—gives rise to the observed Zn(II) affinity.

In conclusion, grafting of the Zn(II)-binding site from human carbonic anhydrase II on the β-barrel of RBP led, first, to increased folding stability in the presence of Zn(II) and permitted, second, the efficient purification of the engineered protein via IMAC. Yet, the binding of retinoic acid, a natural ligand, to RBP was not affected by this modification. Thus, a truly bifunctional binding molecule was obtained, which should provide a promising basis for protein engineering experiments with RBP in the future.

APPENDIX

Influence of Ligand Binding on the Thermodynamics of Protein Folding. A simple two-state equilibrium is assumed between unfolded (U) and folded (F) state of the protein P with an equilibrium constant of folding, K_F

$$P_U \rightleftarrows P_F \qquad K_F = \frac{[P_F]}{[P_U]}$$

and an equilibrium for association of the ligand L with the folded protein

$$P_F + L \rightleftarrows P_F{\cdot}L \qquad K_A = \frac{[P_F{\cdot}L]}{[P_F][L]} = \frac{1}{K_D}$$

where K_A is the association equilibrium constant and K_D is the corresponding constant for dissociation. For the coupled equilibrium it follows that

$$P_U + L \rightleftarrows P_F{\cdot}L \qquad \frac{[P_F{\cdot}L]}{[P_U][L]} = K_F K_A$$

When the Gibbs free energy of folding (which is equal to the free energy of unfolding with reverse sign), ΔG, is determined in an unfolding/refolding experiment (under the assumption that [P] $\ll$ [L], so that the concentration of free L is effectively not influenced by the fraction in complex with P) two cases must be distinguished (Figure 7):

(i) [L] $\ll K_D$, i.e., folded protein is essentially present in the uncomplexed form. In this case, the fraction $[P_F]/[P_U] = K_F$ is measured so that

$$\Delta G = \Delta G_F = -RT \ln K_F$$

(ii) [L] $\gg K_D$, i.e., folded protein is quantitatively present in the ligand-bound form. In this case, the fraction $[P_F{\cdot}L]/[P_U] = K_F K_A[L]$ is measured so that

$$\Delta G = \Delta G_F + \Delta G_A - RT \ln [L]$$

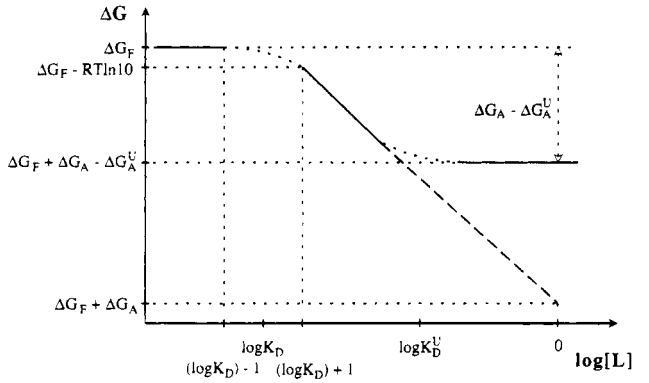

FIGURE 7: Semilogarithmic graph of the free energy of folding, ΔG, as a function of ligand concentration [L]. It is assumed that the protein is either in the fully unbound or the fully bound state if the ligand concentration is at least either 10 times lower or 10 times higher, respectively, than the corresponding dissociation constant. If the unfolded protein does not bind the ligand (case (ii)), ΔG becomes more negative, i. e., folding becomes more stable, with increasing ligand concentration. In this case ΔG equals the sum of ΔG_F and ΔG_A only under thermodynamic reference conditions, i.e., when the active concentration of L is 1 M (broken line).

and the free energy of folding becomes concentration-dependent on L.

If the unfolded protein shows stoichiometric binding of the ligand L as well, the corresponding association equilibrium constant, K_A^U, is defined as follows

$$P_U + L \rightleftarrows P_U{\cdot}L \qquad K_A^U = \frac{[P_U{\cdot}L]}{[P_U][L]} = \frac{1}{K_D^U}$$

Under the plausible assumption that $K_A^U \ll K_A$, i. e., ligand binding to the unfolded protein is weaker than to the folded protein, a third case must be considered:

when (iii) $[L] \gg K_D^U$, i.e., the folded and the unfolded protein are both complexed with the ligand. In this case the fraction $[P_F{\cdot}L]/[P_U{\cdot}L] = K_F K_A / K_A^U$ is measured, so that

$$\Delta G = \Delta G_F + \Delta G_A - \Delta G_A^U$$

and the free energy of unfolding becomes concentration-independent again (see Figure 7).

Only under the latter circumstances the difference in free energy of folding in the absence (case (i)) or presence (case (iii)) of the ligand equals $\Delta\Delta G = \Delta G_A - \Delta G_A^U$, which corresponds to the difference in free energy of ligand binding to the folded and to the unfolded protein, respectively. This situation represents a closed thermodynamic cycle.

Analogous considerations can be made for multiple ligand binding equilibria whereby the important influence of the stoichiometry of ligand binding should be kept in mind. The basic question is in each case which ligand-bound states of the protein are actually populated in the presence of a given ligand concentration during the unfolding/refolding experiment.

REFERENCES

Arnold, F. H., & Haymore, B. L. (1991) *Science 252*, 1796–1797.

Berg, J. M. (1993) *Curr. Opin. Struct. Biol. 3*, 585–588.

Bernstein, F. C., Koetzle, T. F., Williams, G. J. B., Meyer, E. F., Jr., Brice, M. D., Rodgers, J. R., Kennard, O., Shimanouchi, T., & Tasumi, M. (1977) *J. Mol. Biol. 112*, 535–542.

Christianson, D. W. (1991) *Adv. Protein Chem. 42*, 281–355.

Cowan, S. W., Newcomer, M. E., & Jones, T. A. (1990) *Proteins: Struct. Funct. Genet. 8*, 44–61.

Eriksson, A. E., Jones, T. A., & Liljas, A. (1988a) *Proteins: Struct. Funct. Genet. 4*, 274–282.

Eriksson, A. E., Kylsten, P. M., Jones, T. A., & Liljas, A. (1988b) *Proteins: Struct. Funct. Genet. 4*, 283–293.

Fling, S. P., & Gregerson, D. S. (1986) *Anal. Biochem. 155*, 83–88.

Geisselsoder, J., Witney, F., & Yuckenberg, P. (1987) *BioTechniques 5*, 786–791.

Hochuli, E., Bannwarth, W., Döbeli, H., Gentz, R., & Stüber, D. (1988) *Bio/Technology 6*, 1321–1325.

Iverson, B. L., Iverson, S. A., Roberts, V. A., Getzoff, E. D., Tainer, J. A., Benkovic, S. J., & Lerner, R. A. (1990) *Science 249*, 659–662.

Kellis, J. T., Jr., Nyberg, K., & Fersht, A. R. (1989) *Biochemistry 28*, 4914–4922.

Kellis, J. T., Jr., Todd, R. J., & Arnold, F. H. (1991) *Bio/Technology 9*, 994–995.

Liljas, A., Håkansson, K., Jonsson, B. H., & Xue, Y. (1994) *Eur. J. Biochem. 219*, 1–10.

Lindskog, S., & Nyman, P. O. (1964) *Biochim. Biophys. Acta 85*, 462–474.

Martell, A. E., & Smith, R. M. (1974) in *Critical Stability Constants*, Vol. 1, pp 116–119, Plenum Press, New York.

Müller, H. N., & Skerra, A. (1993) *J. Mol. Biol. 230*, 725–732.

Newcomer, M. E., Jones, T. A., Åqvist, J., Sundelin, J., Eriksson, U., Rask, L., & Peterson, P. A. (1984) *EMBO J. 3*, 1451–1454.

Pace, C. N. (1986) *Methods Enzymol. 131*, 266–280.

Pervaiz, S., & Brew, K. (1987) *Fed. Am. Soc. Exp. Biol. 1*, 209–214.

Ponder, J. W., & Richards, F. M. (1987) *J. Mol. Biol. 193*, 775–791.

Regan, L., & Clarke, N. D. (1990) *Biochemistry 29*, 10878–10883.

Sambrook, J., Fritsch, E. F., & Maniatis, T. (1989) *Molecular Cloning: A Laboratory Manual*, Cold Spring Harbor Laboratory Press, Cold Spring Harbor, NY.

Santoro, M. M., & Bolen, D. W. (1988) *Biochemistry 27*, 8063–8068.

Schmidt, T. G. M., & Skerra, A. (1993) *Protein Eng. 6*, 109–122.

Schmidt, T. G. M., & Skerra, A. (1994) *J. Chromatogr. A 676*, 337–345.

Scopes, R. K. (1974) *Anal. Biochem. 59*, 277–282.

Soprano, D. S., & Blaner, W. S. (1994) in *The Retinoids: Biology, Chemistry, and Medicine*, 2nd Ed. (Sporn, M. B., Roberts, A. B., & Goodman, D. S., Eds.) pp 257–281, Raven Press, New York.

Suh, S., Haymore, B. L., & Arnold, F. H. (1991) *Protein Eng. 4*, 301–305.

Tabor, S., & Richardson, C. C. (1987) *Proc. Natl. Acad. Sci. U.S.A. 84*, 4767–4771.

Todd, R. J., van Dam, M. E., Casimiro, D., Haymore, B. L., & Arnold, F. H. (1991) *Proteins: Struct. Funct. Genet. 10*, 156–161.

Veillon, C., & Vallee, B. L. (1978) *Methods Enzymol. 54*, 446–484.

Yanisch-Perron, C., Vieira, J., & Messing, J. (1985) *Gene 33*, 103–119.

Zanotti, G., Berni, R., & Monaco, H. L. (1993a) *J. Biol. Chem. 268*, 10728–10738.

Zanotti, G., Ottonello, S., Berni, R., & Monaco, H. L. (1993b) *J. Mol. Biol. 230*, 613–624.